



Perthamides C–F, potent human antipsoriatic cyclopeptides

Carmen Festa^a, Simona De Marino^a, Valentina Sepe^a, Maria Valeria D'Auria^a, Giuseppe Bifulco^b, Rosa Andrés^c, Maria Carmen Terencio^c, Miguel Payá^c, Cécile Debitus^d, Angela Zampella^{a,*}

^aDipartimento di Chimica delle Sostanze Naturali, Università di Napoli "Federico II", via D. Montesano 49, 80131 Napoli, Italy

^bDipartimento di Scienze Farmaceutiche, Università di Salerno, via Ponte don Melillo, 84084 Fisciano (SA), Italy

^cDepartment of Pharmacology, University of Valencia and Center of Molecular Recognition and Technological Development (IDM), Av. V. Andrés Estelles, s/n 46100 Burjassot, Valencia, Spain

^dInstitut de Recherche pour le Développement (IRD), Polynesian Research Center on Island Biodiversity, BP529, 98713 Papeete, Tahiti, French Polynesia, France

ARTICLE INFO

Article history:

Received 23 May 2011

Received in revised form 5 July 2011

Accepted 26 July 2011

Available online 2 August 2011

Keywords:

Marine compounds

Cyclic peptides

Theonella swinhoei

Anti-inflammatory activity

ABSTRACT

Two new cyclopeptides, perthamides E and F were isolated from the polar extracts of the sponge *Theonella swinhoei*. The new structures, featuring an unprecedented β -amino acid unit (AHMOA), were determined by interpretation of NMR and MS data. The absolute configuration of the AHMOA residue was proposed on the basis of quantum chemical calculation of NMR chemical shifts. Perthamides were proved to inhibit TNF- α and IL-8 release in primary human keratinocytes cells and therefore could represent potentially leads for the treatment of psoriasis.

© 2011 Elsevier Ltd. All rights reserved.

1. Introduction

Psoriasis is a chronic autoimmune inflammatory skin disorder affecting approximately 2–3% of the general population in Europe and North America. Cutaneous and systemic overexpression of various proinflammatory cytokines (TNF- α , IL-8, IFN- γ , etc.) has been demonstrated in psoriatic patients.^{1,2} Notably it has been postulated that TNF- α produced locally in psoriatic lesions creates a TNF- α positive feedback loop that amplifies and sustains the inflammatory process within plaques.³ In fact, recently developed anti-inflammatory therapies based on blocking TNF- α signalling have been shown to be effective in the treatment of psoriasis and could become a highly promising option for the treatment of this skin condition.^{4,5}

Recently, we reported the isolation and the chemical characterization of two cyclic octapeptides, which we named perthamides C (**1**) and D (**2**), from the Solomon marine sponge *Theonella swinhoei*.^{6,7} Perthamide C has an unprecedented primary structure that comprises a 25-membered macrocycle with 6 out the 8 residues constituted by unusual amino acids: γ -methylproline, N^{δ} -carbamoyl- β -OSO₃asparagine, *o*-tyrosine, *D*-Abu, *O*-methylthreonine and the β -amino acid AHMHA (3-amino-2-hydroxy-6-methylheptanoic

acid). Perthamide C (**1**), when tested in a well characterised model of inflammation *in vivo*, i.e., mouse paw oedema, significantly reduced carrageenan-induced paw oedema, displaying a dose-dependent anti-inflammatory activity.

Despite this promising activity, the mechanism of action at the molecular level of perthamide C is unknown. Although the modular peptidic nature and the ready chemical access to perthamide C may open the possibility to investigate new pharmacophores, the isolation of further natural derivatives represents an alternative approach to investigate the structure–activity relationships and to shed light on the biological target of this promise anti-inflammatory lead. In this respect, the sponge *T. swinhoei* (order Lithistida, family Theonellidae), recognized as one of the most prolific sources of bioactive secondary metabolites,⁸ could represent a source of useful perthamide derivatives. Continuing investigation of the polar extracts of this sponge afforded a large amount of perthamide C together with two new derivatives, perthamides E (**3**) and F (**4**).

In this paper we describe the isolation, the structure elucidation including the stereochemical characterization and the biological activity of the new peptides (Fig. 1).

2. Results and discussion

The lyophilized sponge (400 g) was extracted with MeOH, and the combined extracts were fractionated according to the Kupchan

* Corresponding author. Tel.: +39 081 678525; fax: +39 081 678552; e-mail addresses: angela.zampella@unina.it, azampell@unina.it (A. Zampella).

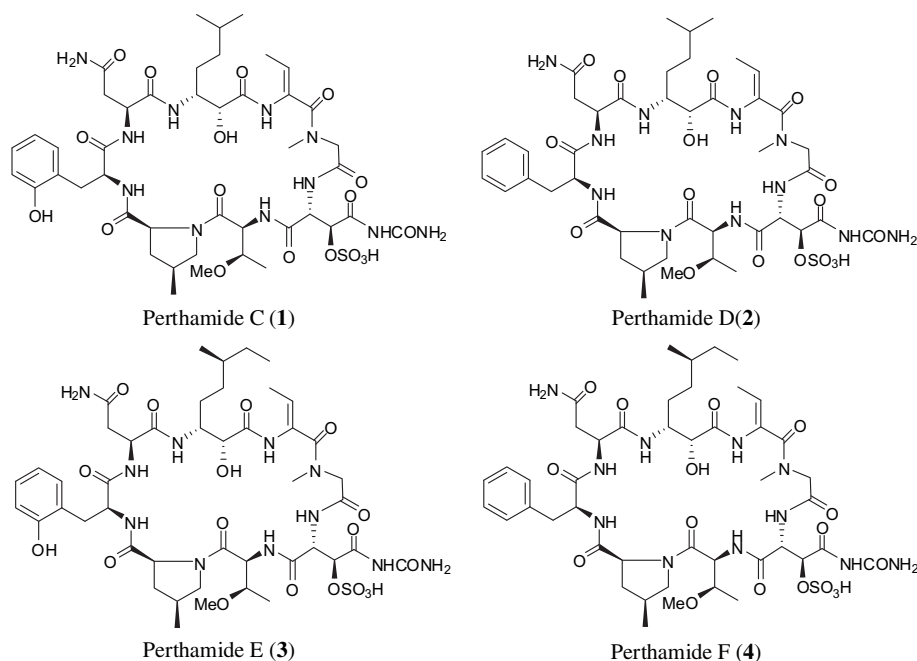


Fig. 1.

partitioning procedure.⁹ The *n*-BuOH extract was purified by DCCC (*n*-BuOH/Me₂CO/H₂O, descending mode) followed by reverse-phase HPLC to afford perthamides C–F.

Perthamide E (**3**) was isolated as a colourless amorphous solid and showed the pseudomolecular ion peak at *m/z* 1080.4361 [M–H][–] in the HRESIMS spectrum, corresponding to the molecular formula C₄₅H₆₇N₁₁O₁₈S and indicating the presence of one additional carbon atom with respect to perthamide C (**1**).

A careful analysis of the NMR data (Table 1), including COSY, HSQC, TOCSY, indicated the presence of the same α -amino acid residues found in **1** and a variation of the β -amino acid unit

(AHMHA in perthamide C). Even if from ¹H NMR and HSQC data an additional methylene group with respect to perthamide C was easily detected (δ_C 28.7, δ_H 1.03, 1.22), the analysis of the proton spin system of this amino acid unit was not straightforward due to the heavy overlap in the ¹H NMR high field region and to the absence of some scalar coupling in the COSY spectrum. The ¹H and ¹³C NMR resonances of C-1/C-5 nuclei relative to this portion were almost superimposable with the corresponding values found for the 3-amino-2-hydroxy-6-methylheptanoic acid (AHMHA) residue in perthamide C. Additionally, inspection of ¹H NMR spectrum indicated the presence of one methyl doublet (0.74, d, *J*=6.2 Hz) and

Table 1
NMR data (700 MHz, DMSO-*d*₆) of perthamides E (**3**) and F (**4**)

Position	Perthamide E (3)		Position	Perthamide F (4)	
	δ_H (J in Hz) ^a	δ_C ^a		δ_H (J in Hz) ^a	δ_C ^a
<i>ThrOMe</i>			<i>ThrOMe</i>		
1	—	170.9	1	—	170.9
2	4.91d (9.5)	55.4	2	4.81d (9.6)	55.4
3	4.16m	72.9	3	4.14–4.22m	72.9
4	1.23d (5.9)	14.3	4	1.21d (5.8)	14.4
OMe	3.26s	54.7	OMe	3.25s	54.5
NH	9.01d (9.1)		NH	8.90d (8.8)	
γ MePro			γ MePro		
1	—	170.7	1	—	170.7
2	3.89dd (11.1, 6.6)	63.4	2	3.98dd (11.0, 6.7)	63.3
3	0.71m, 2.05–2.13m	36.2	3	1.09 ovl, 2.14–2.18m	36.3
4	2.20–2.30m	33.2	4	2.19–2.27m	33.5
5	3.39 ovl, 4.11 ovl	53.2	5	3.38 ovl, 4.10 ovl	53.2
6	1.03d (5.8)	15.8	6	1.01d (5.7)	15.6
<i>o</i> -Tyr			<i>Phe</i>		
1	—	170.6	1	—	170.6
2	4.11 ovl	56.4	2	4.28–4.36m	55.8
3	2.86dd (13.2, 3.2), 2.93t (13.2)	30.7	3	2.83dd (13.5, 3.5), 3.14 ovl	36.2
1'	—	124.3	1'	—	137.8
2'	—	154.6	2'	7.19d (7.4)	128.0
3'	6.87d (7.8)	114.5	3'	7.30t (7.4)	128.3
4'	7.10t (7.8)	128.0	4'	7.22d (7.3)	126.3
5'	6.80t (7.3)	119.9	5'	7.30t (7.4)	128.3
6'	7.16 ovl	130.5	6'	7.19d (7.4)	128.0
NH	7.20 ovl		NH	6.91d (8.0)	

(continued on next page)

Table 1 (continued)

Perthamide E (3)			Perthamide F (4)		
Position	δ_{H} (J in Hz) ^a	δ_{C} ^a	Position	δ_{H} (J in Hz) ^a	δ_{C} ^a
OH	10.1s		OH	—	
Asn			Asn		
1	—	170.4	1	—	170.4
2	4.67–4.71m	48.0	2	4.66 br s	47.9
3	2.41d (16.3), 3.14dd (16.3, 4.7)	36.8	3	2.43d (16.0), 3.15 ovl	36.8
4	—	172.6	4	—	172.5
NH	7.19 ovl		NH	7.12 ovl	
NH ₂	6.52 br s, 7.83 br s		NH ₂	6.55 br s, 7.80 br s	
AHMOA			AHMOA		
1	—	169.8	1	—	169.8
2	4.14 ovl	72.8	2	4.12 ovl	72.9
3	4.01t (9.9)	51.9	3	4.01t (9.8)	52.0
4	1.09m, 1.41–1.47m	23.6	4	1.07 ovl, 1.36–148m	23.5
5	1.06m	31.8	5	1.04m	31.6
6	1.17m	33.4	6	1.19m	33.3
7	1.03m, 1.22 ovl	28.7	7	1.05m, 1.23m	28.8
8	0.76t (7.0)	11.0	8	0.77t (6.9)	11.1
9	0.74d (6.2)	18.5	9	0.75d (6.2)	18.4
NH	6.37d (9.1)		NH	6.43d (9.0)	
OH	4.81 br s		OH	4.81 br s	
d-Abu			d-Abu		
1	—	167.5	1	—	167.4
2	—	132.3	2	—	132.1
3	5.77q (6.8)	126.5	3	5.75q (6.5)	126.0
4	1.54d (6.8)	12.0	4	1.54d (6.5)	12.0
NH	8.62s		NH	8.66s	
NMeGly			NMeGly		
1	—	167.2	1	—	167.2
2	3.31d (17.5), 4.19d (17.5)	51.5	2	3.30 ovl, 4.18d (17.0)	51.6
NMe	2.70s	34.6	NMe	2.70s	34.6
N ^δ -c-β-OSO ₃ Asn			N ^δ -c-β-OSO ₃ Asn		
1	—	167.5	1	—	167.2
2	5.04t (7.3)	53.0	2	5.01t (7.3)	52.9
3	4.59d (7.1)	74.9	3	4.58d (6.9)	75.0
4	—	170.5	4	—	170.5
βNH	7.16 ovl		βNH	7.15 ovl	
NH	8.89s		NH	8.93s	
CO	—	n.o	CO	—	n.o
NH ₂	7.29 br s, 7.51 br s		NH ₂	7.33 br s, 7.50 br s	

Ovl: overlapped; n.o: not observed.

^a ¹H and ¹³C assignments aided by COSY, TOCSY, HSQC and HMBC experiments.

one methyl triplet (0.76, t, *J*=7.0 Hz) that replaced the two highly overlapped methyl doublet signals at δ_{H} 0.77 and 0.78 observed in the ¹H NMR spectrum of **1**, suggesting the presence of a terminal appendage for this unit different from the isopropyl group located on AHMHA.

Two spin systems, a CH–CH₃ (δ_{H} 1.17, δ_{C} 33.4, C-6; δ_{H} 0.74, δ_{C} 18.5, C-9) and a CH₂–CH₃ (δ_{H} 1.03, 1.22, δ_{C} 28.7, C-7; δ_{H} 0.76, δ_{C} 11.0, C-8) were disclosed from COSY and HSQC data (Fig. 2). Even if no COSY correlation was observed between the proton at δ_{H} 1.17 (H-6) and protons ascribable to the methylene at C-7, the connection between C-6 and C-7 was inferred by HMBC data as shown in Fig. 2, defining a *sec*-butyl subunit. The linkage of this latter with the methylene carbon at C-5 (δ_{C} 31.8, δ_{H} 1.06) was deduced from the diagnostic heteronuclear long range correlation between the methyl protons at δ_{H} 0.74 (C-9) with the carbon resonance at δ_{C} 31.8 (C-5). Definitive confirmation to the above unit derived from 2D-TOCSY analysis that showed correlations starting from H-9 to H-3.

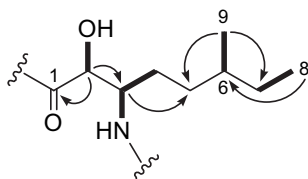


Fig. 2. AHMOA unit in perthamides E and F with COSY/TOCSY connectivities (bold bonds) and HMBC correlations (arrows).

Therefore the new 3-amino-2-hydroxy-6-methyloctanoic acid (AHMOA) unit, which is also unprecedented in natural peptides, was established in perthamide E.

As shown in Fig. 3, the sequence of the amino acids in perthamide E (**3**) was established on the basis of careful analysis of ROESY data and was proved to be the same found in **1**.

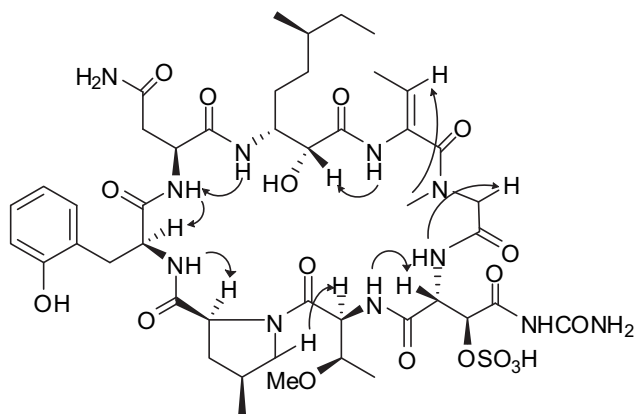


Fig. 3. Selected ROE correlations for perthamide E.

The close resemblance of ¹H and ¹³C NMR chemical shifts of all α -amino acid residues with the corresponding values of perthamide C suggested that they have the same configuration. To confirm

this hypothesis, **3** was subjected to the same procedures described for the stereochemical characterization of the amino acid residues in perthamide C,^{6,7} establishing the presence of L-Asn, L-*o*-Tyr, *cis*-L- γ MePro, L-ThrOMe, *erythro*-D-N⁰-c- β -OSO₃Asn and Z-D-Abu.

As concern AHMOA, this unit has an additional stereogenic centre with respect to AHMHA in perthamide C. Chemical shifts and the homonuclear coupling constant pattern of C-2/C-3 centres closely matched with those of the corresponding centres in AHMHA for which the 2*R*,3*R* absolute configuration was established by stereoselective synthesis.⁷ The impossibility to relate this stereotriad to C-6 through the intervening of two methylene carbon that showed highly overlapped proton resonances, hampered the application of *J*-based analysis to define the stereochemistry at C-6.

Starting from the encouraging results recently obtained from our research group in the solving of stereochemical ambiguities on marine natural products from *T. swinhoei*,^{10,11} we decided to apply quantum chemical (QM) calculation of the NMR chemical shifts^{12,13} to establish the absolute configuration of AHMOA residue in **3**.

Two diastereoisomers of perthamide E (**3a** and **3b**, Fig. 4) were built, varying the configuration at C-6 of AHMOA residue and fixing the absolute configuration of all residues previous established by Marfey's analysis with perthamide C as standard.

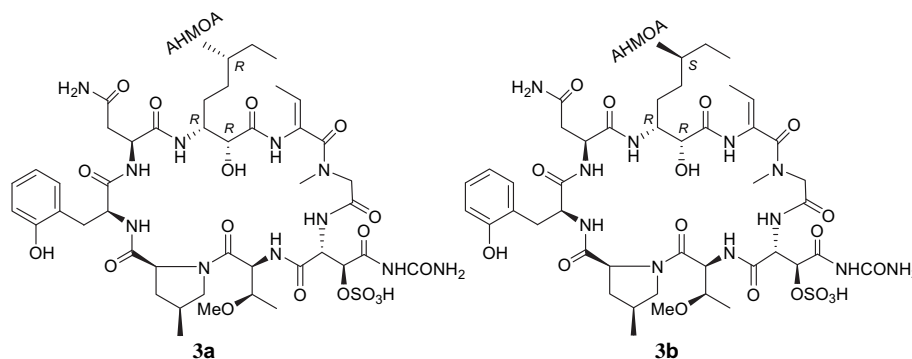


Fig. 4. AHMOA-C6 epimers (**3a,b**) of perthamide E (**3**).

The adopted protocol consists of four fundamental steps: (a) conformational search and preliminary geometry optimization of all the significantly populated conformers of each stereoisomer; (b) geometry optimization of all the species at MPW1PW91 level; (c) GIAO ¹³C and ¹H NMR calculations of all the so obtained structures; (d) comparison of the Boltzmann averaged ¹³C and ¹H NMR chemical shifts calculated for each stereoisomer with those measured for perthamide E.

The preliminary conformational search was performed by empirical force field molecular dynamics (OPLS force field, Macro-model 8.5 software).¹⁴ A set of distance restraints were collected from 2D-ROESY NMR experiments (*t*_{mix}=150 ms) and used in molecular dynamics calculations (500 K) of two diastereoisomers.

Subsequently, all the conformers found were optimised at DFT level by using the MPW1PW91 functional and 6-31G(d) basis set. By discarding all of the conformations higher in energy than a threshold of 10 kcal/mol from the most stable species, five major conformers were found for stereoisomer **3a** and five for **3b**. These showed a well defined macrocycle core, but differed in the conformational structure of the side chain of AHMOA residue (Fig. 5).

Finally, GIAO ¹³C and ¹H chemical shift calculations were performed at the MPW1PW91 functional and 6-31G(d,p) basis set on each set of conformers relative to the epimers **3a,b**, and calculated by simulating the presence of DMSO (IEF-PCM),¹⁵ using Gaussian 09 software.¹⁶ For each stereoisomer, the ¹³C and ¹H chemical shifts were obtained as the weighted average chemical shift values in all of the conformers sampled by the initial conformational search. MAE (Mean Absolute Error) parameters were obtained for each of

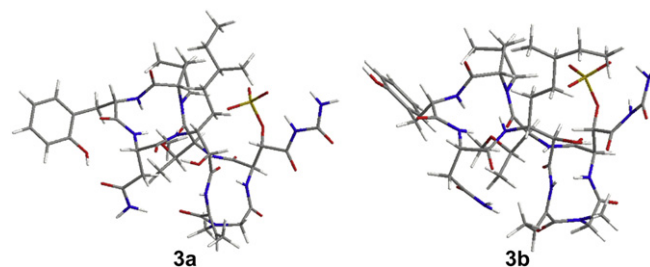


Fig. 5. NMR solution state representative conformations for **3a** and **3b** obtained by restrained MD calculations, using ROESY data collected at 700 MHz in DMSO-*d*₆.

the two diastereoisomers. Through evaluation of the MAE values, the GIAO calculated ¹³C and ¹H NMR chemical shifts of nuclei of AHMOA residue indicated the best fit between stereoisomer 2*R*,3*R*,6*S* (**3b**) and the experimental data.

Even though small differences in the MAE values of calculated ¹³C chemical shifts were observed (4.2 for **3a** vs 3.9 for **3b**, Table 2), MAE values of calculated ¹H chemical shifts were relatively enough different (0.40 for **3a** vs 0.24 for **3b**, Table 3) to propose the 2*R*,3*R*,6*S* absolute configuration for AHMOA residue. Definitive confirmation

to the above tentatively assigned absolute configuration could derive from synthetic studies already ongoing in our laboratories.

Table 2

Experimental and calculated ¹³C NMR chemical shifts (ppm), $\Delta\Delta$ [$(\delta_{\text{calcd}} - \delta_{\text{exptl}})$], $\Delta\Delta_{\text{abs}}$ [$(|\delta_{\text{calcd}} - \delta_{\text{exptl}}|)$] and MAE (Mean average error as $\sum[|\delta_{\text{exptl}} - \delta_{\text{calcd}}|/n]$) on selected sp³ atoms of AHMOA residue in **3**

	2 <i>R</i> ,3 <i>R</i> ,6 <i>R</i>				2 <i>R</i> ,3 <i>R</i> ,6 <i>S</i>			
	δ_{exptl}	δ_{calcd}	$\Delta\Delta$	$\Delta\Delta_{\text{abs}}$	δ_{calcd}	$\Delta\Delta$	$\Delta\Delta_{\text{abs}}$	
C2	72.8	78.7	-5.9	5.9	77.3	-4.5	4.5	
C3	51.9	58.8	-6.9	6.9	53.2	-1.3	1.3	
C4	23.6	31.6	-8.0	8.0	36.8	-13.2	13.2	
C5	31.8	38.5	-6.7	6.7	31.6	0.2	0.2	
C6	33.4	34.1	-0.7	0.7	36.5	-3.1	3.1	
C7	28.7	30.7	-2.0	2.0	32.3	-3.6	3.6	
C8	11.0	14.2	-3.2	3.2	14.0	-3.0	3.0	
C9	18.5	18.7	-0.2	0.2	21.5	-3.0	3.0	
$\sum[\delta_{\text{exptl}} - \delta_{\text{calcd}}]$			-33.6	33.6		-31.5	31.9	
$\sum[\delta_{\text{exptl}} - \delta_{\text{calcd}} /n]$			-4.2			-3.9		
MAE ^a				4.2			3.9	

^a Mean average error = $\sum[|\delta_{\text{exptl}} - \delta_{\text{calcd}}|/n]$.

Perthamide F (**4**) showed a molecular weight 16 mass units (one oxygen atom) smaller than that of perthamide E (**3**). The ¹H NMR spectrum, which is very similar to that of **3**, clearly revealed the absence of the signal ascribable to exchangeable OH proton located on the *o*-Tyr residue in perthamides C and E and a perturbation in the aromatic region.

Table 3

Experimental and calculated ^1H NMR chemical shifts (ppm), $\Delta\Delta$ [$(\delta_{\text{calcd}} - \delta_{\text{exptl}})$], $\Delta\Delta_{\text{abs}}$ [$(\delta_{\text{calcd}} - \delta_{\text{exptl}})$] and MAE (Mean average error as $\sum |(\delta_{\text{exptl}} - \delta_{\text{calcd}})|/n$) on selected sp^3 atoms of AHMOA residue in **3**

	2R,3R,6R				2R,3R,6S		
	δ_{exptl}	δ_{calcd}	$\Delta\Delta$	$\Delta\Delta_{\text{abs}}$	δ_{calcd}	$\Delta\Delta$	$\Delta\Delta_{\text{abs}}$
H2	4.14	4.18	-0.04	0.04	4.36	-0.22	0.22
H3	4.01	3.88	0.13	0.13	4.03	-0.02	0.02
H4a	1.09	1.96	-0.87	0.87	1.60	-0.51	0.51
H4b	1.44	2.26	-0.82	0.82	1.77	-0.33	0.33
H5	1.06	1.29	-0.23	0.23	1.54	-0.48	0.48
H6	1.17	1.94	-0.77	0.77	1.22	-0.05	0.05
H7a	1.03	0.92	0.11	0.11	1.40	-0.37	0.37
H7b	1.22	1.86	-0.64	0.64	1.10	0.12	0.12
H8	0.76	0.99	-0.23	0.23	0.91	-0.15	0.15
H9	0.74	0.92	-0.18	0.18	0.85	-0.11	0.11
$\sum \delta_{\text{exptl}} - \delta_{\text{calcd}} $			-3.5	4.0		-2.1	2.4
$\sum (\delta_{\text{exptl}} - \delta_{\text{calcd}}) /n$			-0.35			-0.21	
MAE ^a				0.40			0.24

^a Mean average error = $\sum |(\delta_{\text{exptl}} - \delta_{\text{calcd}})|/n$.

Interpretation of 2D NMR data, including COSY, HSQC and HMBC data (Table 1) indicated that perthamide F (**4**) possesses similar primary structure to that of perthamide E (**3**), with the differences traced to substitution of *o*-Tyr in **3** with Phe in **4**. As for in perthamide E, the presence of L-Asn, L-Phe, *cis*-L- γ MePro, L-ThrOMe, *erythro*-D- N^{δ} -c- β -OSO₃Asn was established by application of Marfey's method,¹⁷ whereas the complete agreement of chemical shifts and coupling constant pattern of AHMOA and D-Abu residues suggested the same configuration.

Starting from the anti-inflammatory activity demonstrated for perthamide C, we decided to investigate the eventual antipsoriatic effect of these natural compounds on TNF- α and IL-8 release in primary human keratinocytes (PHK) cells (Fig. 6).

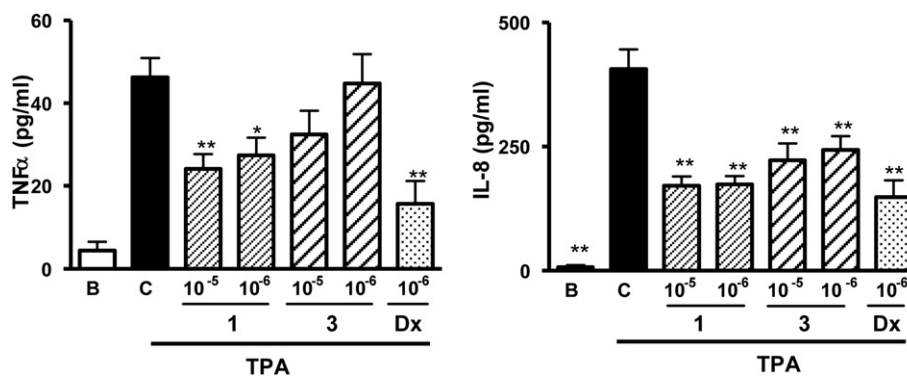


Fig. 6. Dose-dependent inhibition of TNF- α and IL-8 production by perthamide C (**1**) and E (**3**) in PHK cells. B: non stimulated cells. C: stimulated cells. Dx: Dexamethasone.

Dexamethasone, a well known antipsoriatic drug, was used as a reference tool. Perthamides C and E were devoid of significant cytotoxic effects on PHK cells at concentrations up to 10 μM , as assessed by the mitochondrial-dependent reduction of 3-(4,5-dimethylthiazol-2-yl)-2,5-diphenyltetrazolium bromide (MTT) to formazan (data not shown). Their ability to inhibit TNF- α and IL-8 release on PHK cells stimulated with 12-*O*-tetradecanoylphorbol-13-acetate (TPA) was also investigated (Fig. 6). Interestingly, perthamide C (**1**) showed a dose-dependent capability to inhibit TNF- α and IL-8 release, whereas perthamide E (**3**) significantly inhibited only IL-8 release. The ability of perthamide C to inhibit both key biomarkers upregulated in the inflammatory response of psoriatic skin, could be interesting to provide promising antipsoriatic agents.

In conclusion in this paper we report the isolation and the stereostructural characterization of two new cyclic peptides from the marine sponge *T. swinhoei*.

Moreover we demonstrated that perthamides C and E are endowed with anti-inflammatory activity mediated via up-regulation of TNF- α , a key cytokine in inflammatory skin diseases, such as psoriasis.

3. Experimental section

3.1. General experimental procedures

Specific rotations were measured on a Jasco P-2000 polarimeter. The melting points were measured on a Büchi Melting Point B-440 apparatus. IR spectra were recorded on a Perkin–Elmer FT-IR 100 spectrometer. High-resolution ESIMS spectra were performed with a Micromass QTOF spectrometer. ESIMS experiments were performed on an Applied Biosystem API 2000 triple-quadrupole mass spectrometer. NMR spectra were obtained on Varian Inova 500 and Varian Inova 700 NMR spectrometers (^1H at 500 and 700 MHz, ^{13}C at 125 and 175 MHz, respectively) equipped with a Sun hardware, δ (ppm), J in Hz, spectra referred to DMSO- d_6 as internal standard (δ_{H} 2.50, δ_{C} 39.5). HPLC was performed using a Waters 510 pump equipped with Waters Rheodine injector and a differential refractometer, model 401.

Through-space ^1H connectivities were evidenced using a ROESY experiment with mixing time of 150 ms.

DCCC was performed using a DCC-A (Rikakikai Co. Di Tokyo) equipped with 250 columns (internal diameter 3 mm).

The purities of compounds were determined to be greater than 95% by HPLC, MS and NMR.

3.2. Sponge material and separation of individual peptides

T. swinhoei (order Lithistida, family Theonellidae) was collected at a depth of 22 m, on an isolated reef off the western coast of

Malaita Island, Solomon Islands, in July 2004. The samples were frozen immediately after collection and lyophilized to yield 400 g of dry mass. Taxonomic identification was performed by Dr John Hooper at Queensland Museum, Brisbane, Australia, where a voucher specimen is deposited under the accession number G322662.

The lyophilized material (400 g) was extracted with methanol ($3 \times 1.5\text{L}$) at room temperature and the crude methanolic extract was subjected to a modified Kupchan's partitioning procedure as follows. The methanol extract was dissolved in a mixture of MeOH/H₂O containing 10% H₂O and partitioned against *n*-hexane (15.2 g). The water content (% v/v) of the MeOH extract was adjusted to 30% and partitioned against CHCl₃ (5.83 g). The aqueous phase was concentrated to remove MeOH and then extracted with *n*-BuOH (6.0 g).

The *n*-BuOH extract (6.0 g) was chromatographed in three runs by DCCC using *n*-BuOH/Me₂CO/H₂O (3:1:5) in the descending mode

(the upper phase was the stationary phase), flow rate 8 mL/min; 4 mL fractions were collected and combined on the basis of their similar TLC retention factors.

Fractions 6–12 (1.1 g) were purified in many runs by HPLC on a reverse phase C-12 Jupiter Proteo column (Phenomenex, 4 μ , 250 \times 4.6 mm, 1.0 mL/min), eluting in isocratic mode with 59% MeOH/H₂O (0.1% TFA) to afford 265.3 mg of perthamide C (t_R =3.5 min) and 10.5 mg of perthamide E (t_R =6.9 min).

Fractions 13–14 (113 mg) were purified by HPLC on a reverse phase C-12 Jupiter Proteo column (Phenomenex, 4 μ , 250 \times 4.6 mm, 1.0 mL/min), with 59% MeOH/H₂O (0.1% TFA). The peak at t_R =6.9 min was analyzed by ¹H NMR and revealed a mixture of perthamides E and F. This mixture was purified by HPLC on Vydac C-18 column (5 μ , 250 \times 4.6 mm, 1.0 mL/min) with 24% MeCN/H₂O as eluent to give 2.3 mg of perthamide E (t_R =6.3 min) and 1.7 mg of perthamide F (t_R =8.4 min).

3.3. Characteristic data for each peptide

3.3.1. Perthamide C (1). White amorphous solid; $[\alpha]_D^{22}$ –87.7 (c 0.87, MeOH); IR ν_{max} (KBr disc)/cm⁻¹ 3395, 2932, 1665, 1618, 1522, 1457, 1234, 1130, 1083, 1028; mp 210.8–214.6 °C; HRESIMS m/z 1066.4106 [M–H]⁻ (calcd for C₄₄H₆₄N₁₁O₁₈S: 1066.4151).

3.3.2. Perthamide E (3). White amorphous solid; $[\alpha]_D^{22}$ –199.6 (c 0.22, MeOH); IR ν_{max} (KBr disc)/cm⁻¹ 3395, 2950, 1670, 1618, 1533, 1457, 1251, 1130, 1080, 1031; mp 204.1–211.6 °C; ¹H and ¹³C NMR data in DMSO-*d*₆ given in Table 1; HRESIMS m/z 1080.4361 [M–H]⁻ (calcd for C₄₅H₆₆N₁₁O₁₈S m/z 1080.4308).

3.3.3. Perthamide F (4). White amorphous solid; $[\alpha]_D^{22}$ –10.5 (c 0.07, MeOH); ¹H NMR and ¹³C NMR data in DMSO-*d*₆ given in Table 1; HRESIMS m/z 1064.4313 [M–H]⁻ (calcd for C₄₅H₆₆N₁₁O₁₇S m/z 1064.4359).

3.4. Determination of amino acid absolute configuration

3.4.1. Hydrolysis of perthamides. Perthamides (500 μ g) C–F were dissolved, respectively, in 0.5 mL of 6 N HCl in three evacuated glass tubes and heated at 160 °C for 16 h. The solvent was removed in vacuo and the resulting material was subjected to further derivatisation.

3.4.2. LC–MS analysis of Marfey's (FDAA) derivatives. A portion of the hydrolysate mixture (300 μ g) was dissolved in 80 μ L of a 2:3 solution of TEA/MeCN and this solution was then treated with 75 μ L of 1% 1-fluoro-2,4-dinitrophenyl-5-L-alaninamide (L-FDAA) in 1:2 MeCN/Me₂CO. The vials were heated at 70 °C for 1 h, and the contents were neutralised with 0.2 N HCl (50 μ L) after cooling to room temperature. An aliquot of the L-FDAA derivative was dried under vacuum, diluted with MeCN–5% HCOOH in H₂O (1:1) and separated on a Proteo C18 column (25 \times 1.8 mm i.d.) by means of a linear gradient from 10% to 50% aqueous MeCN containing 5% formic acid and 0.05% trifluoroacetic acid, over 45 min at 0.15 mL/min. The RP-HPLC system was connected to the electrospray ion source by inserting a splitter valve and the flow going into the mass spectrometer source was set at a value of 100 μ L/min. Mass spectra were acquired in positive ion detection mode (m/z interval of 320–900) and the data were analyzed using the suite of programs Xcalibur; all masses were reported as average values. The capillary temperature was set at 280 °C, capillary voltage at 37 V, tube lens offset at 50 V and ion spray voltage at 5 V.

All FDAA derivatives of amino acid residues in perthamide E were co-eluted with the corresponding ones in perthamide C.⁶

To determine the absolute configuration of Phe residue in perthamide F, an authentic sample of perthamide D was used as

a standard. The hydrolysate of perthamide F contained L-Phe (45.0 min).

3.5. Computational details

Molecular mechanics (MM) calculations were performed using MacroModel 8.5¹⁴ and the MMFFs force field OPLS. MonteCarlo Multiple Minimum (MCMM) method (10,000 steps) was used in order to extensively explore the conformational space. All the structures, so obtained, were optimised using the Polak-Ribiere Conjugated Gradient algorithm (PRCG, 1000 steps, maximum derivative less than 0.05 kcal/mol). The initial geometries of the minimum energy conformers were optimised at the hybrid DFT MPW1PW91 level using the 6-31G(d) basis set (Gaussian 09 software).¹⁶ GIAO ¹³C and ¹H NMR chemical shifts were performed using the MPW1PW91 functional, the 6-31G(d, p) basis set and DMSO as solvent, using as input the geometry previously optimised at MPW1PW91/6-31G(d) level.

3.6. Anti-inflammatory assays

3.6.1. Isolation, culture and stimulation of primary human keratinocytes (PHK). Foreskins from healthy young males were the source of primary human keratinocytes. All protocols and procedures were approved by the Institutional Ethical Committee. Isolation of keratinocytes was performed essentially as described by Boyce and Ham;¹⁸ briefly, skin samples were washed, cut, scraped, and treated with a disperse solution to prepare a largely epidermal layer. The tissue was then trypsinized, filtered, centrifuged, and the resultant keratinocytes cultured and seeded as required. The cells were incubated at 37 °C in a humidified atmosphere of 5% CO₂ in a serum-free low-Ca²⁺ (<0.1 mM) defined Keratinocyte-SFM (Invitrogen). The medium was changed every other day. For all experiments, cells were seeded at passage numbers 1–3 into 24-well plates (25 \times 10⁵ cells per well) and were treated upon reaching 70–90% confluence. Before the experiments, cells were grown in basal medium without growth factors for 24 h to avoid the effects of supplements in the growth medium and to obtain quiescent cells with low levels of activated NF- κ B. Prior to the addition of the stimulus, the basal medium was renewed (300 μ L) and the cells were subjected to 30 min pretreatment with perthamide C or perthamide E. 12-O-Tetradecanoylphorbol-13-acetate (TPA) (Sigma–Aldrich) 1 μ g/mL was then added to the culture and the cells were incubated for 7 h after which the supernatant was removed and stored at 20 °C until further use. The MTT assay was performed to the remaining cells to test the effect of the compounds on cell viability.

3.7. Cytotoxicity evaluation (MTT assay)

Cytotoxicity of the tested compounds was determined by the 3-(4,5-dimethylthiazol-2-yl)-2,5-diphenyltetrazolium bromide (MTT) uptake method as described.¹⁹ Briefly, at the end of the incubation period (7 h), culture medium was withdrawn. The cell culture was incubated for 1 h at 37 °C and in the dark with 200 μ L of MTT at 0.5 mg/mL in basal medium. Formazan violet crystals, induced by MTT cleavage by mitochondrial enzymes, were dissolved in DMSO and analyzed by spectrophotometry at λ =490 nm.

3.8. ELISA assays

Human TNF- α levels in cell supernatants were measured using an ELISA kit from R&D Systems. IL-8 ELISA kit was from Bender MedSystems. Both ELISA analyses were performed in accordance with the manufacturer's instructions.

3.9. Statistical analysis

The results are presented as meanSEM and n represents the number of experiments. The level of statistical significance was determined by analysis of variance (ANOVA) followed by Dunnett's *t*-test for multiple comparisons.

Acknowledgements

NMR spectra were provided by the CSIAS, Centro Interdipartimentale di Analisi Strumentale, Faculty of Pharmacy, University of Naples. We thank the Solomon Islands government for collection permits, the Fisheries Department, R. Sulu (University of the South Pacific in Honiara) for their help and assistance, and Dr. John Hooper for the identification of the sponges. R.M.A. was the recipient of a research fellowship from Generalitat Valenciana (BFPI/2009/145). This work was supported in part by the Spanish Ministry of Science and Innovation (SAF2009-10347).

References and notes

- Schottelius, A. J.; Moldawer, L. L.; Dinarello, C. A.; Asadullah, K.; Sterry, W.; Edwards, C. K. *Exp. Dermatol.* **2004**, *13*, 193–222.
- Young, C. N.; Koepke, J. I.; Terlecky, L. J.; Borkin, M. S.; Boyd Savoy, L.; Terlecky, S. R. *J. Invest. Dermatol.* **2008**, *128*, 2606–2614.
- Banno, T.; Gazel, A.; Blumenberg, M. J. *Biol. Chem.* **2004**, *279*, 32633–32642.
- Asadullah, K.; Volk, H. D.; Sterry, W. *Trends Immunol.* **2002**, *23*, 47–53.
- Gottlieb, A. B. *J. Am. Acad. Dermatol.* **2005**, *53*, S3–S16.
- Festa, C.; De Marino, S.; Sepe, V.; Monti, M. C.; Luciano, P.; D'Auria, M. V.; Debitus, C.; Bucci, M.; Vellecco, V.; Zampella, A. *Tetrahedron* **2009**, *65*, 10424–10428.
- Sepe, V.; D'Auria, M. V.; Bifulco, G.; Ummarino, R.; Zampella, A. *Tetrahedron* **2010**, *66*, 7520–7526.
- Wegerski, C. J.; Hammond, J.; Tenney, K.; Matainaho, T.; Crews, P. *J. Nat. Prod.* **2007**, *70*, 89–94.
- Kupchan, S. M.; Britton, R. W.; Ziegler, M. F.; Sigel, C. W. *J. Org. Chem.* **1973**, *38*, 178–179.
- Festa, C.; De Marino, S.; Sepe, V.; D'Auria, M. V.; Bifulco, G.; Debitus, C.; Bucci, M. R.; Vellecco, V.; Zampella, A. *Org. Lett.* **2011**, *13*, 1532–1535.
- De Marino, S.; Sepe, V.; D'Auria, M. V.; Bifulco, G.; Renga, B.; Petek, S.; Fiorucci, S.; Zampella, A. *Org. Biomol. Chem.* **2011**, *9*, 4856–4862.
- Bifulco, G.; Dambrosio, P.; Gomez-Paloma, L.; Riccio, R. *Chem. Rev.* **2007**, *107*, 3744–3779.
- Di Micco, S.; Chini, M. G.; Riccio, R.; Bifulco, G. *Eur. J. Org. Chem.* **2010**, 1411–1434.
- MacroModel, Version 8.5*; Schrödinger LLC: New York, NY, 2003.
- Cances, E.; Mennucci, B.; Tomasi, J. *J. Chem. Phys.* **1997**, *107*, 3032–3041.
- Frisch, M. J.; Trucks, G. W.; Schlegel, H. B.; Scuseria, G. E.; Robb, M. A.; Cheeseman, J. R.; Scalmani, G.; Barone, V.; Mennucci, B.; Petersson, G. A.; Nakatsujii, H.; Caricato, M.; Li, X.; Hratchian, H. P.; Izmaylov, A. F.; Bloino, J.; Zheng, G.; Sonnenberg, J. L.; Hada, M.; Ehara, M.; Toyota, K.; Fukuda, R.; Hasegawa, J.; Ishida, M.; Nakajima, T.; Honda, Y.; Kitao, O.; Nakai, H.; Vreven, T.; Montgomery, J. A., Jr.; Peralta, J. E.; Ogliaro, F.; Bearpark, M.; Heyd, J. J.; Brothers, E.; Kudin, K. N.; Staroverov, V. N.; Kobayashi, R.; Normand, J.; Raghavachari, K.; Rendell, A.; Burant, J. C.; Iyengar, S. S.; Tomasi, J.; Cossi, M.; Rega, N.; Millam, N. J.; Klene, M.; Knox, J. E.; Cross, J. B.; Bakken, V.; Adamo, C.; Jaramillo, J.; Gomperts, R.; Stratmann, R. E.; Yazyev, O.; Austin, A. J.; Cammi, R.; Pomelli, C.; Ochterski, J. W.; Martin, R. L.; Morokuma, K.; Zakrzewski, V. G.; Voth, G. A.; Salvador, P.; Dannenberg, J. J.; Dapprich, S.; Daniels, A. D.; Farkas, Ö.; Foresman, J. B.; Ortiz, J. V.; Cioslowski, J.; Fox, D. J. *Gaussian 09, Revision A.02*; Gaussian: Wallingford CT, 2009.
- Marfey, P. *Carlsberg Res. Commun.* **1984**, *49*, 591–596.
- Boyce, S. T.; Ham, R. G. *J. Tissue Cult. Methods* **1985**, *9*, 83–93.
- Borenfreund, E.; Babick, H.; Martin-Alguacil, N. *Toxicol. in Vitro* **1988**, *2*, 1–6.